



**HAL**  
open science

## Fission of 1 A GeV $^{238}\text{U}$ -ions on a hydrogen-target

M. Bernas, P. Napolitani, F. Rejmund, C. Stéphan, J. Taieb, L. Tassan-Got,  
P. Armbruster, T. Enqvist, M.-V. Ricciardi, K.-H. Schmidt, et al.

► **To cite this version:**

M. Bernas, P. Napolitani, F. Rejmund, C. Stéphan, J. Taieb, et al.. Fission of 1 A GeV  $^{238}\text{U}$ -ions on a hydrogen-target. Seminar on Fission- Pont d'Oye V, Sep 2003, Habay-la-Neuve, Belgium. pp.223-231. in2p3-00024868

**HAL Id: in2p3-00024868**

**<https://hal.in2p3.fr/in2p3-00024868>**

Submitted on 10 Oct 2005

**HAL** is a multi-disciplinary open access archive for the deposit and dissemination of scientific research documents, whether they are published or not. The documents may come from teaching and research institutions in France or abroad, or from public or private research centers.

L'archive ouverte pluridisciplinaire **HAL**, est destinée au dépôt et à la diffusion de documents scientifiques de niveau recherche, publiés ou non, émanant des établissements d'enseignement et de recherche français ou étrangers, des laboratoires publics ou privés.

**THE DISTRIBUTION OF COLLISION PRODUCTS IN THE  
THE REACTION OF 1 A GeV  $^{238}\text{U}$ -IONS ON A  
HYDROGEN-TARGET**

M. BERNAS, P. NAPOLITANI, F. REJMUND, C. STEPHAN, J. TAIEB,  
L. TASSAN-GOT

*I.P.N. d'Orsay, F-91406 Orsay Cedex, France  
E-mail: bernas@ipno.in2p3.fr*

P. ARMBRUSTER, T. ENQVIST, M.-V. RICCIARDI, K.-H. SCHMIDT  
*G.S.I. Darmstadt, D-64291 Darmstadt, Germany*

J. BENLLIURE, E. CASAJEROS, J. PEREIRA  
*Univ. of Santiago de Compostela, E-15706 Santiago, Spain*

A. BOUDARD, R. LEGRAIN, S. LERAY, C. VOLANT  
*DAPNIA/SPhN CEA/Saclay F-91191 Gif-sur-Yvette Cedex, France*

S. CZAJKOWSKI  
*DAPNIA/SPhN CENBG, IN2P3 F-33175 Gradignan, France*

The production cross sections and the kinematical properties of fission fragment residues have been studied in the reaction  $^{238}\text{U}$  (1 A.GeV) + p. Isotopic distributions were measured for all elements from O ( $Z = 8$ ) to Gd ( $Z = 64$ ). The distribution of fission velocities and of production cross sections as function of  $Z$  of the fragments, provide relevant informations on the intermediate fissioning nuclei.

## 1. Introduction

The spallation and fission of the excited nuclei produced in collisions of 1 A.GeV U on a hydrogen target has been investigated in order to extend the domain of data already obtained by our collaboration, namely Au + p<sup>1,2</sup> and Pb + p<sup>3</sup> to a fissile projectile. These studies are part of an experimental program to collect nuclear data relevant for ADS<sup>4,5</sup>, RNB and spallation neutron sources. For technical applications, reliable and

accurate cross sections are needed and a special care was devoted to the experiment in order to fulfill these requirements. We report here on the measurement of fission residues left after the cascade of nucleon-nucleon collisions induced by the proton in the U-nucleus. The excited fragments produced cool down by evaporation of nucleons or light particles and may undergo fission. Evaporation residues have been analysed in a parallel work <sup>6</sup>. The experimental set up used at GSI is briefly described and the main results are presented. We show how from the kinematical properties and the isotopic distribution of fission fragments (f.f), the intermediate fissioning parent nucleus can be inferred. The balance between evaporation residues and f.f. provides a test of the energy dissipation of the excited intermediate system.

## 2. Experiment

Using inverse kinematics at relativistic energy, the f.f. are totally stripped of their electrons and forward focused. They can be separated by the FRagment Separator (FRS) <sup>7</sup> and identified by the associated detection system i.e. an ionisation chamber and a time of flight for Z and A determination, respectively. The performances of the equipment were demonstrated by the identification of 117 new n-rich fission fragments in U (0.75 GeV) + Be collisions. <sup>8,9</sup>

The systematic scanning of the FRS magnetic rigidity allows to reconstruct the center of mass velocity spectra, truncated by the FRS angular acceptance  $\alpha$ , as shown in Fig. 1b. Note that 4 to 5 isotopes of all of the 36 elements populated by fission are scanned simultaneously. It reduces the relative uncertainties due to beam intensity calibration or dead time corrections. The laboratory velocity of f.f. results from the Lorentz addition of the projectile velocity with the fission velocity.

From the gap between the first momenta of the two peaks, that is twice the apparent velocity  $V_{app}$ , knowing  $\alpha$  and its variance  $\sigma_\alpha$ , we calculate the angular transmission and the fission velocity  $V_f$  for each isotope, see <sup>10</sup>.

## 3. Kinematics

Fission velocities varies as the inverse of the atomic number Z due to momentum conservation in fission. For each element, velocities of 15 to 25 isotopes are investigated. They decrease slightly with the mass of the isotope (1 to 2 %) except for the 4 lightest isotopes where they drop by 10 to 20%. This fall confirms that the 4 lightest isotopes are produced by

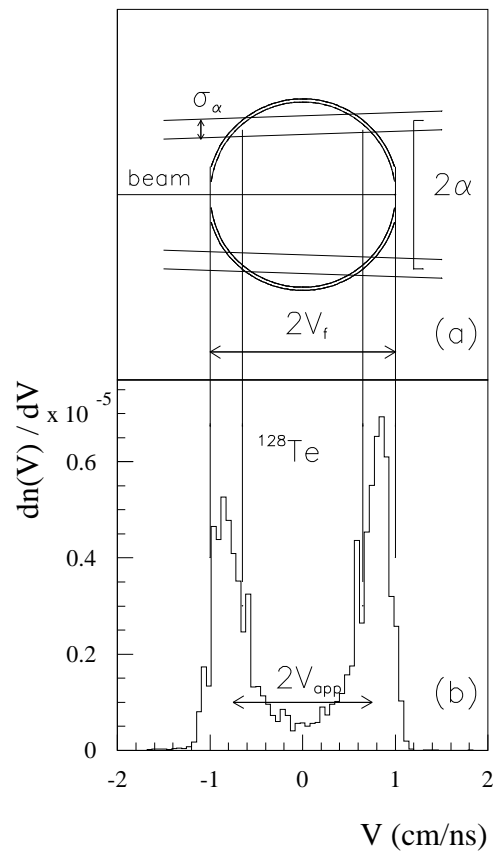


Figure 1. a) Schematic view of the experimental parameters shaping the measured velocity spectrum in the frame of the fissioning system.  $V_f$  is the fission-fragment velocity,  $\alpha$  is the angular acceptance of the FRS, and  $\sigma_\alpha$  its variance. b) Velocity spectrum of  $^{128}\text{Te}$  in the frame of the fissioning system. The velocity  $V = 0$  refers to the projectile frame.  $V_{app}$  is the apparent fission velocity defined in the text.

secondary break-up of heavier fission fragments<sup>11</sup>.

A mean value of the velocity per element is presented on Fig. 2, to-

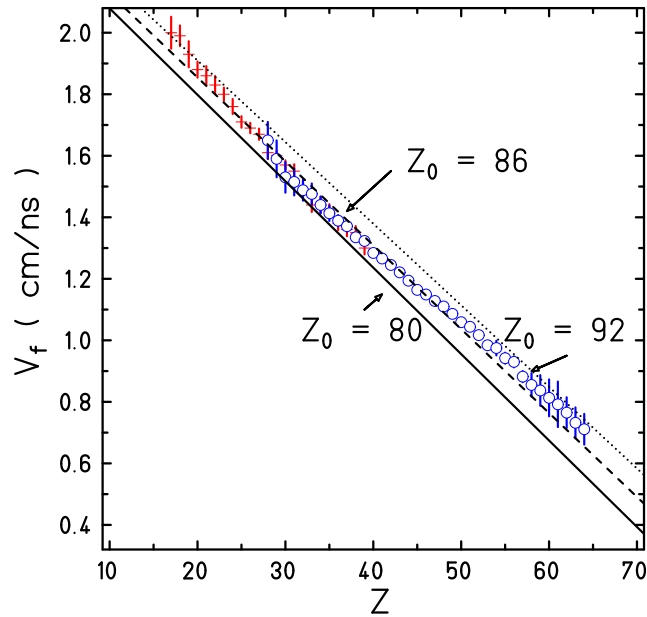


Figure 2. Fission fragment velocities as a function of  $Z$ . The lines are obtained using the calculation of velocity for fissioning parent nuclei of  $Z_0 = 80$  (full line),  $Z_0 = 86$  (dashed line) and  $Z_0 = 92$  (dotted line) with the parametrisation of ref. 12 and 13 and a deformation of  $\beta = 0.65$  for both fragments.

gether with the 3 straight lines expected in case of fission of U, Rn and Hg. The parameterization of <sup>12,13</sup> and a deformation of  $\beta = 0.65$  is assumed for calculating the three distributions of velocity as a function of  $Z$  of the f.f.. A small decrease of the measured values relative to the expected slope for decreasing  $Z$  is found. The data are compatible with  $84 < Z < 90$  for the fissioning nuclei.

#### 4. Isotopic Yields: Symmetric and asymmetric fission

Isotopic cross sections have been obtained for all isotopes of the 36 elements produced by U + p fission, down to a threshold value of 0.1 mb. They cover a range of 0.1 to 14 mb. The measurements can be extended further for neutron-rich isotopes since they are not contaminated by secondary break-up, contrary to cross sections on the neutron-deficient side. Three distributions are shown here on Fig. 3 to illustrate our results. A systematic uncertainty of 10% is calculated, mostly due to the beam monitoring. The

error bars reported on Fig. 3 correspond to the relative uncertainties.

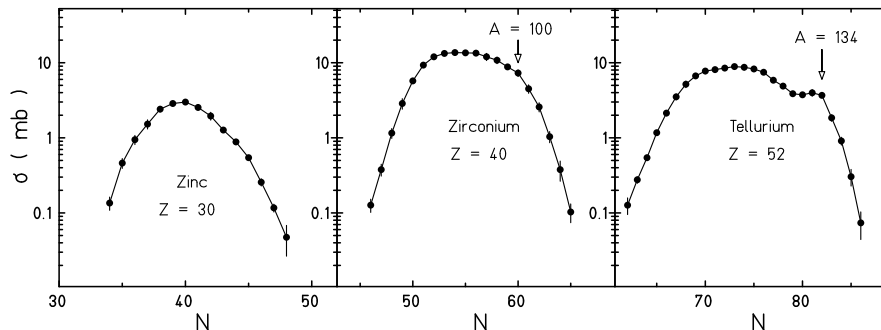


Figure 3. Isotopic cross sections for fission-fragments in the reaction  $^{238}\text{U} + 1 \text{ AGeV } p$  for elements  $_{30}\text{Zn}$ ,  $_{40}\text{Zr}$  and  $_{52}\text{Te}$ . The arrows indicate a pair of isotopes, the production of which is enhanced in asymmetric fission.

The isotopic cross section distributions show a bell shape with a shoulder on the neutron-rich side, more prominent in case of isotopes strongly populated in asymmetric fission. The "asymmetric" regime of fission, has been analysed in various experiments. In our previous study of  $\text{U} + \text{Pb}$  fission for example <sup>14</sup>, it was enhanced due to the strong Coulomb excitation of the giant resonance. The mean value of the mass  $A$ ,  $\overline{A}(Z)$  and the width  $\sigma_A(Z)$  were determined coherently with previous works. The isotopic distributions presently measured are decomposed into contributions of symmetric and asymmetric fissions. As a result the element distribution shown on Fig. 4a can be shared into both components, as shown on the figure.

The mean value of  $Z$ ,  $\overline{Z} = 45$ , is calculated for the total of the distribution shown on Fig.4a, down to  $Z = 28$ . For  $Z < 28$ , the binary break-up is still observed, and assigned by the FRS kinematical selection <sup>15</sup>. The occurrence of the very asymmetric break-up with rising cross sections was already observed and discussed in other systems at similar excitation energies <sup>16</sup>.

The region populated by the two fission regimes are characterized on the Fig. 4b. Asymmetric fission populates a narrow corridor ( $\sigma_N^Z = 1.8$ ) in the neutron-rich region, ( $\overline{N}/Z = 1.52$ ). The symmetric process drives in a region of less neutron-rich isotopes, towards the valley of stability, where  $\overline{N}/Z$  ( $\approx 1.3$ ) increases slowly with  $Z$ , crossing the valley at  $Z = 57$ , as shown

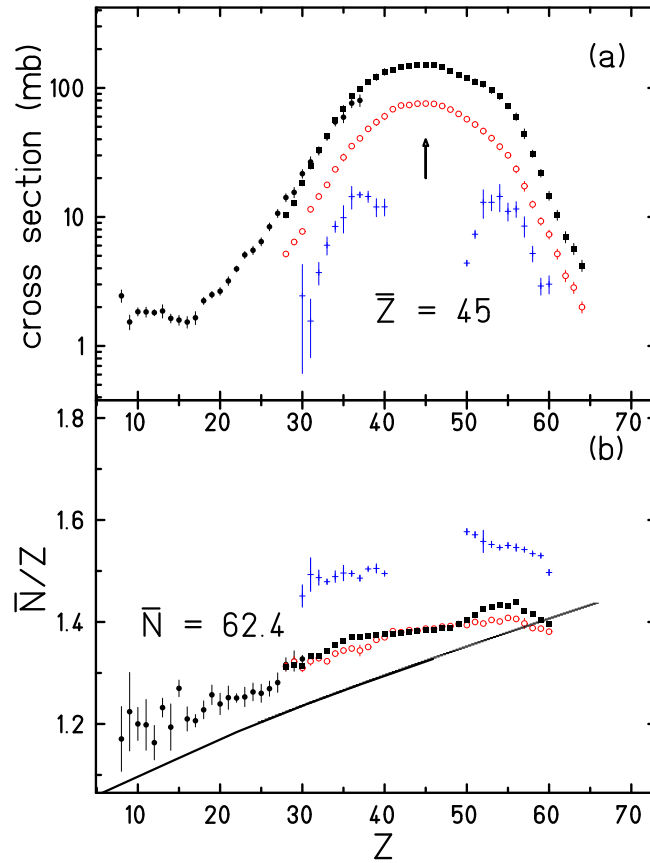


Figure 4. a) Distribution of f.f. integrated over  $N$  for  $^{238}\text{U} + p$  at 1 A.GeV (Full points or squares). Light circles: symmetric fission, and dashes: asymmetric component (with large error bars). In order to single out the symmetric component, the related values have been divided by a factor of 2. b) Mean neutron number divided by  $Z$  as a function of  $Z$  for the total distribution and for symmetric and asymmetric fission.

on Fig. 4b and  $\sigma_N^Z$  increases from 2 for  $Z = 30$  to 4 for  $Z = 60$ .

From the mean values of the atomic numbers of f.f.  $\bar{Z} = 45$  and from the mean neutron number  $\bar{N} = 63$  the most probable symmetric fission leads to two f.f. of  $^{108}\text{Rh}$ . A mean fissioning parent nucleus can be reconstructed using the conservation of protons and neutrons in the spallation process and the energy balance between the cascade and the evaporation chain ending in fission. The mean cascade in  $^{238}\text{U}$  induced by the protons leads

to a  $^{232}\text{Th}$  excited at  $E^* = 183$  MeV after 3 protons and 4 neutrons have been torn away from the incident system. Then a mean number of 11 neutrons are evaporated to reach a  $^{221}\text{Th}$  at  $E^* = 149$  MeV. With a mean number of 5 post fission neutrons emitted, the two symmetric f.f. of  $^{108}\text{Rh}$  are obtained. This estimation is based on known energies required to free neutrons and protons in the cascade and on binding energies of neutrons in the evaporation process. The simulations to be done still, will substantiate the result.

The fission cross section is calculated by summing elemental cross sections  $\sigma(Z)$  over the whole fission area. For symmetric and asymmetric fission, cross sections of  $(1.42 \pm 0.15)$  b and of  $(0.105 \pm 0.01)$  b are found, respectively. The total fission cross section amounts to  $(1.53 \pm 0.15)$  b, a value which compares well with the results of direct measurements of fission cross sections  $(1.46 \pm 0.07)$  b and  $(1.48 \pm 0.06)$  b<sup>17,18</sup>, respectively.

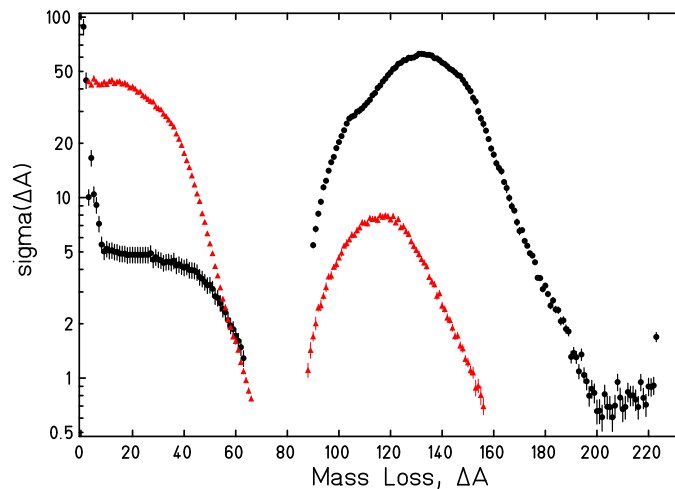


Figure 5. Comparison of cross-sections for evaporation and fission residues as a function of the mass-loss  $\Delta A$  for the two collision systems Pb + p (triangles) and U + p (full points) at 1 A GeV.

## 5. Mass Yields: Comparison with the Pb (1 A GeV)+ p system

The mass distribution  $\sigma(A)$  is built by summing isotopic cross sections for  $A$  fixed. It shows a roughly symmetric Gaussian shape except for the

shoulders of asymmetric fission. We have plotted on Fig. 5 cross sections as function of the mass loss for spallation residues and f.f.. The Pb + p results <sup>3</sup> are reported also to illustrate the importance of the fissility in case of U. Total cross sections are almost the same within 10 %, (see the Table) but the dominant contribution of the fission for U is inhibited in case of Pb, whereas for Pb, excited fragments cool down mainly by neutron evaporation.

reaction	$\sigma_{tot}$ (barn)	$\sigma_{fis}$ (barn)	$\sigma_{EVR}$ (barn)
U + p	$1.99 \pm 0.17$	$1.53 \pm 0.13$	$0.46 \pm 0.08$
Pb + p	$1.84 \pm 0.23$	$0.16 \pm 0.07$	$1.68 \pm 0.22$

Simulations have been performed by our collaboration to reproduce the measured f.f. cross sections. The best result is obtained by using a calculation of the cascade with a new version of INCL <sup>19</sup>, the statistical de-excitation code ABLA <sup>20,21</sup>, and a fission parametrization PROFI <sup>22</sup>

The cross sections for (U + p)-evaporation residues <sup>6</sup> cannot be reproduced by the Bohr and Wheeler model and dissipation has to be included in the calculation. The reproduction of measured data is optimum with a dissipation constant  $\beta = 2 \cdot 10^{21} \text{ s}^{-1}$  <sup>23</sup>.

## 6. Conclusion

The isotopic cross sections are determined for 1300 isotopes produced in the reaction U (1 AGeV) + p see Fig. 6. The fission fragments, separated kinematically from the spallation residues are investigated and production cross-sections are determined within a range of 2 to 3 orders of magnitude down to 10 to 100  $\mu\text{b}$  with an accuracy better than 15 %. The kinetic energy of each fragment is determined. Of a total cross section of 2 barns, 77 % is attributed to fission and 23 % to evaporation residues. Multifragmentation can be neglected. The mean element number and the mean neutron number of the f.f. allow to reconstruct <sup>221</sup>Th as the mean parent fissioning nucleus.

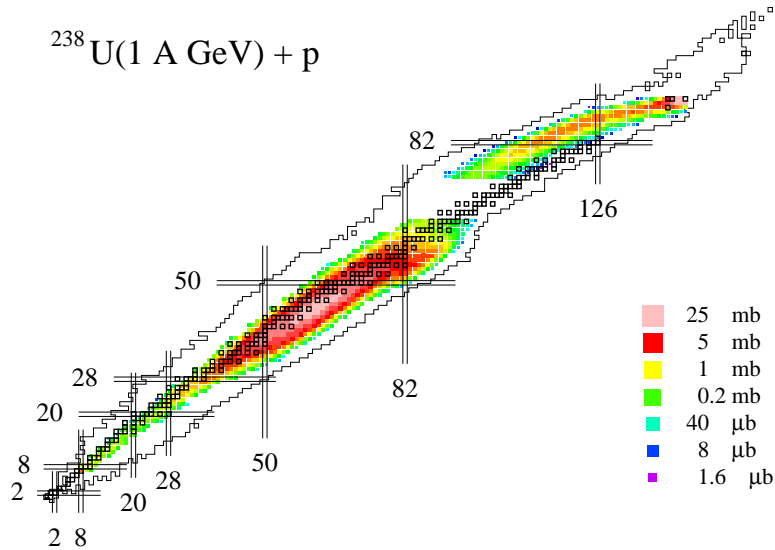


Figure 6. Two-dimensional plot of the isotopic cross sections for fission fragments (ref 10 et 15) and evaporation residues (ref 6) obtained in 1 A GeV  $^{238}\text{U} + \text{p}$  shown on the chart of isotopes with indication of the stable isotopes. Increasing dark level correspond to decreasing cross sections according to the logarithmic scale indicated.

## References

1. F. Rejmund et al. *Nucl. Phys.***A683** 481 (2001)
2. J. Benlliure et al. Seminar on fission, Pont d'Oye IV 223 (1999)
3. T. Enqvist et al. *Nucl. Phys.***A686** 481 (2001)
4. F. Carminati, R. Klapisch, J. P. Revol, Ch. Roche, J. A. Rubio, C. Rubbia. CERN Report CERN/AT/93-47(ET), (1993).
5. G. Fioni, see the contribution therein.
6. J. Taieb, PhD Thesis Univ. Paris XI (2000) IPNO-T-00-10 and J. Taieb et al. *Nucl. Phys.* **A724** 413 (2003)
7. H. Geissel et al. *Nucl. Instrum. Methods***B70** 286 (1992).
8. M. Bernas et al. *Phys. Lett.***415B** 111 (1997)
9. Ch. Engelmann, Thesis Univ. Tübingen (1998), GSI Rep. Diss. 1998-15, and *Zeit. Phys.***A352** 351 (1995)
10. M. Bernas et al. *Nucl. Phys.***725A** 213 (2003)

11. P. Napolitani et al. *Nucl. Phys.***727A** 120 (2003)
12. B.D. Wilkins, E.P. Steinberg, R.R. Chasman, *Phys. Rev.***C14** 1832 (1976)
13. C. Böckstiegel et al. *Phys. Lett.***398B** 259 (1997)
14. C. Donzaud *Eur. Phys. J.***A1** 407 (1998)
15. M. V. Ricciardi et al. proceedings of the XXXIX Int. Winter Meeting on Nucl. Phys., Bormio, Italy (2001).  
M. V. Ricciardi, PhD Thesis in progress, GSI-Darmstadt.
16. D.G. Sarantites et al. *Phys. Lett.***218B** 427 (1989)
17. B. A. Bochagov et al. *Sov. J. Nucl. Phys.***28-2** 291 (1978)
18. L. A. Vaishnene et al. *Z. Phys.***302A** 143 (1981)
19. A. Boudard, J. Cugnon, S. Leray and C. Volant, *Phys. Rev.***66C** 044615 (2002)
20. J.-J. Gaimard and K.-H. Schmidt *Nucl. Phys.***531A** 709 (1991)
21. A. R. Junghans et al. *Nucl. Phys.***629A** 635 (1998)
22. J. Benlliure et al. *Nucl. Phys.***628A** 458 (1998)
23. B. Jurado, PhD Thesis, Univ. Compostela (2002) and GSI Rep. 2002-10, to be published